



# Muon–electron conversion in a family gauge boson model



Yoshio Koide<sup>a</sup>, Masato Yamanaka<sup>b,\*</sup>

<sup>a</sup> Department of Physics, Osaka University, Toyonaka, Osaka 560-0043, Japan

<sup>b</sup> Maskawa Institute, Kyoto Sangyo University, Kyoto 603-8555, Japan

## ARTICLE INFO

### Article history:

Received 8 August 2016

Accepted 1 September 2016

Available online 6 September 2016

Editor: N. Lambert

## ABSTRACT

We study the  $\mu$ – $e$  conversion in muonic atoms via an exchange of family gauge boson (FGB)  $A_2^1$  in a  $U(3)$  FGB model. Within the class of FGB model, we consider three types of family-number assignments for quarks. We evaluate the  $\mu$ – $e$  conversion rate for various target nuclei, and find that next generation  $\mu$ – $e$  conversion search experiments can cover entire energy scale of the model for all of types of the quark family-number assignments. We show that the conversion rate in the model is so sensitive to up- and down-quark mixing matrices,  $U^u$  and  $U^d$ , where the CKM matrix is given by  $V_{\text{CKM}} = U^{u\dagger}U^d$ . Precise measurements of conversion rates for various target nuclei can identify not only the types of quark family-number assignments, but also each quark mixing matrix individually.

© 2016 The Authors. Published by Elsevier B.V. This is an open access article under the CC BY license (<http://creativecommons.org/licenses/by/4.0/>). Funded by SCOAP<sup>3</sup>.

## 1. Introduction

The idea of family gauge bosons (FGBs)  $A_i^j$  ( $i, j = 1, 2, 3$ ) seems to be the most natural extension of the standard model (SM). In the SM of quarks and leptons, a degree of freedom which is not yet accepted as a gauge symmetry is only that of the families (generations). So far, because of the severe constraint from the observed  $P^0$ – $\bar{P}^0$  mixing ( $P = K, D, B, B_s$ ) it has been considered that a scale of the FGBs is very large so that we cannot observe those at terrestrial experiments.

Against such conventional models, a FGB model on a low energy scale has been proposed by Sumino [1,2]. The model has the following characteristics (details are given in Sec. 2): (i) Family symmetry  $U(3)$  is broken at a low energy scale of  $\mathcal{O}(10^3)$  TeV. (ii) The FGB mass matrix is diagonal in the flavor basis in which the charged lepton mass matrix is diagonal, so that lepton family-number violation does not occur. (iii) FGB masses and gauge coupling  $g_F$  are not free parameters. FGB masses and  $g_F$  are related to the charged lepton masses and to the electroweak gauge coupling, respectively. Hence the predictions in the model are less ambiguous.

There is a variety of types of FGB spectrum and quark family-number assignments. We focus on three models compatible with observed  $P^0$ – $\bar{P}^0$  mixing. In Model A, FGB masses have an inverted hierarchy, i.e., lightest and heaviest FGB are  $A_3^3$  and  $A_1^1$ , respec-

tively [3]. In Model B, the quark family-number is assigned as twisted, e.g.,  $(d_1, d_2, d_3) = (b, s, d)$  (Model B<sub>1</sub>), and  $(d_1, d_2, d_3) = (b, d, s)$  (Model B<sub>2</sub>) for  $(e_1, e_2, e_3) \equiv (e^-, \mu^-, \tau^-)$  [4].

Our interest is in how to confirm the FGB model at terrestrial experiments. We have already pointed out a possibility that we observe the lightest FGB  $A_1^1$  in Model B at the LHC [5]. There is however still a possibility that the FGB is too heavier to observe at the LHC. Now it is worth investigating how to check such too heavy FGBs.

In this paper, we focus on  $\mu$ – $e$  conversion in muonic atoms. The FGB  $A_2^1$  possesses a muon- and electron-number violating interaction, and gives rise to the  $\mu$ – $e$  conversion, but not other muon-number violating decays. New experiments to search for the  $\mu$ – $e$  conversion will launch soon, e.g., DeeMe, COMET, Mu2e, and PRISM experiment, whose single event sensitivities are  $B(\text{Si}) \sim 5 \times 10^{-14}$  (DeeMe) [6],  $B(\text{Al}) \sim 3 \times 10^{-17}$  (COMET and Mu2e) [7,8], and  $B(\text{Al}) \sim 7 \times 10^{-19}$  (PRISM) [7]. Here  $B(N)$  denotes branching ratio of the  $\mu$ – $e$  conversion with a target nucleus  $N$ . We evaluate the  $\mu$ – $e$  conversion rate, and show that these experiments scan entire parameter space of the model. Once  $\mu$ – $e$  conversion events are discovered, we need to find out the  $A_2^1$  contribution in the events without relying on other muon-number violating observables. And, with only the  $\mu$ – $e$  conversion signals, we need to discriminate the FGB model from other models in which the  $\mu$ – $e$  conversion is dominant muon-number violating process [9–13]. We discuss the discrimination through the measurement of the branching ratios for various nuclei.

The precise measurement of the branching ratios plays an important role. The branching ratios in the model are sensitive to

\* Corresponding author.

E-mail addresses: [koide@kuno-g.phys.sci.osaka-u.ac.jp](mailto:koide@kuno-g.phys.sci.osaka-u.ac.jp) (Y. Koide), [masato.yamanaka@cc.kyoto-su.ac.jp](mailto:masato.yamanaka@cc.kyoto-su.ac.jp) (M. Yamanaka).

**Table 1**  
Three extended FGB models.  $q^0$  stands for eigenstates of the  $U(3)$  family gauge symmetry. Note that this lower bound on  $M_{12}$  is derived from  $P^0-\bar{P}^0$  mixing measurements [4], not from  $\mu-e$  conversion search experiments.

	Model A	Model B <sub>1</sub>	Model B <sub>2</sub>
Symmetries	$U(3) \times U(3)'$	$U(3) \times U(3)'$	$U(3) \times U(3)'$
lepton currents	$\bar{\ell}_L^i \gamma_\mu \ell_j$	$\bar{\ell}_L^i \gamma_\mu \ell_{jL} - \bar{\ell}_{jR} \gamma_\mu \ell_R^i$	$\bar{\ell}_L^i \gamma_\mu \ell_{jL} - \bar{\ell}_{jR} \gamma_\mu \ell_R^i$
quark currents	$\bar{q}^{0i} \gamma_\mu q_j^0$	$\bar{q}^{0i} \gamma_\mu q_j^0$	$\bar{q}^{0i} \gamma_\mu q_j^0$
$g_F/\sqrt{2}$	$0.491/\sqrt{n}$	$0.428/\sqrt{n}$	$0.428/\sqrt{n}$
$(e_1, e_2, e_3)$	$(e^-, \mu^-, \tau^-)$	$(e^-, \mu^-, \tau^-)$	$(e^-, \mu^-, \tau^-)$
$(d_1, d_2, d_3)$	$(d^0, s^0, b^0)$	$(b^0, s^0, d^0)$	$(b^0, d^0, s^0)$
$M_{11} : M_{22} : M_{33}$	$(1/m_e)^{n/2} : (1/m_\mu)^{n/2} : (1/m_\tau)^{n/2}$	$m_e^{n/2} : m_\mu^{n/2} : m_\tau^{n/2}$	$m_e^{n/2} : m_\mu^{n/2} : m_\tau^{n/2}$
lower bound of $M_{12}$ ( $n=1$ )	$1.76 \times 10^3$ [TeV]	98.4 [TeV]	98.0 [TeV]
lower bound of $M_{12}$ ( $n=2$ )	$1.80 \times 10^4$ [TeV]	78.2 [TeV]	77.9 [TeV]

the quark mixing matrices  $U^u$  and  $U^d$ , where Cabibbo–Kobayashi–Maskawa (CKM) matrix is given by  $V_{\text{CKM}} = U^{u\dagger} U^d$  [14]. We have chance to individually determine  $U^u$  and  $U^d$  through the measurements of the  $\mu-e$  conversion. We will discuss the feasibility of it.

This work is organized as follows. First we briefly review the FGB model. We illustrate three types of quark family-number assignments. Then we introduce four types of quark mixing to describe the interaction between FGBs and quarks. Next, in Sec. 3, we formulate the  $\mu-e$  conversion rate in the FGB model. In Sec. 4, we give numerical results, and show that the FGB model can be confirmed or ruled out at  $\mu-e$  conversion search experiments in near future. We discuss feasibility for discriminations among three types of quark family-number assignments and four types of quark mixing matrices. Sec. 5 is devoted to summarize this work.

## 2. Family gauge boson model

Let us give a brief review of a  $U(3)$  family gauge boson (FGB) model proposed by Sumino [1]. Sumino has noticed a problem in a charged lepton mass relation [15],

$$K \equiv \frac{m_e + m_\mu + m_\tau}{(\sqrt{m_e} + \sqrt{m_\tau} + \sqrt{m_\tau})^2} = \frac{2}{3}. \quad (2.1)$$

The relation is satisfied by the pole masses,  $K^{\text{pole}} = (2/3) \times (0.999989 \pm 0.000014)$ , but not so well satisfied by the running masses,  $K(\mu = m_Z) = (2/3) \times (1.00189 \pm 0.00002)$ . The running masses  $m_{e_i}(\mu)$  are given by [16]

$$m_{e_i}(\mu) = m_{e_i} \left[ 1 - \frac{\alpha_{em}(\mu)}{\pi} \left( 1 + \frac{3}{4} \log \frac{\mu^2}{m_{e_i}^2(\mu)} \right) \right]. \quad (2.2)$$

In the absence of family-number dependent factor  $\log(m_{e_i}^2)$ , the running masses  $m_{e_i}(\mu)$  also satisfy the relation (2.1). In order to understand this puzzle, Sumino has proposed a  $U(3)$  FGB model so that a factor  $\log(m_{e_i}^2)$  from the QED correction is canceled by the FGB loop contribution  $\log(M_{ij}^2)$  [1]. Here, the masses of FGBs  $A_i^j$ ,  $M_{ij}$ , are given by

$$M_{ij}^2 = k(m_{e_i}^n + m_{e_j}^n), \quad (2.3)$$

where  $k$  is a constant with dimension of  $(\text{mass})^{2-n}$ . The cancellation mechanism holds for any  $n$ , because  $\log M_{ij}^n = n \log M_{ij}$ . The original model has studied the  $n=1$  case [1]. The cancellation requires the following relation between the family gauge coupling  $g_F$  and QED coupling  $e$ ,

$$\left( \frac{g_F}{\sqrt{2}} \right)^2 = \frac{2}{n} e^2 = \frac{4}{n} \left( \frac{g_w}{\sqrt{2}} \right)^2 \sin^2 \theta_w. \quad (2.4)$$

Here  $\theta_w$  is the Weinberg angle. Note that the cancellation mechanism holds only at the one loop level. Sumino has speculated the scale of  $U(3)$  family symmetry is an order of  $10^3$  TeV [1,2].

In the FGB model, the family symmetry is broken by a scalar  $\Phi$  with  $(\mathbf{3}, \mathbf{3})$  of  $U(3) \times O(3)$ . The family-numbers of quarks and leptons, which are triplets of  $U(3)$ , are changed only by exchanging  $\Phi \bar{\Phi}$ , not the single  $\Phi$ . Thus, the FGB contribution to pseudo-scalar meson oscillations is highly suppressed. The FGB mass matrix is diagonal in the flavor basis in which the charged lepton mass matrix is diagonal, because those masses are generated by the common scalar  $\Phi$ . Therefore, family-number violation does not occur in the charged lepton sector.

In the original model, charged leptons ( $e_{Li}, e_{Ri}$ ) are assigned to  $(\mathbf{3}, \mathbf{3}^*)$  of  $U(3)$  family symmetry, which makes the sign of FGB loop correction to be opposite to the QED correction for the cancellation. So the original model is not anomaly free. In order to avoid this anomaly problem, Yamashita and one of the authors (YK) have proposed an extended FGB model [3]: two scalars  $\Psi$  and  $\Phi$  are introduced, which are  $(\mathbf{3}, \mathbf{3}^*)$  of  $U(3) \times U(3)'$ . Charged lepton masses are generated via the VEV of  $\Phi$  only. FGB masses are achieved via the VEVs of  $\Phi$  and  $\Psi$ . Relations of these VEVs are  $\langle \Psi \rangle \propto \langle \Phi \rangle^{-1}$  and  $\langle \Psi \rangle \gg \langle \Phi \rangle$ . These relations lead the FGB spectrum (2.3) with negative  $n$ , in contrast to the original FGB model in which a VEV of single scalar field generates both of masses of charged leptons and FGBs. We can therefore realize the cancellation with a normal assignment  $(e_{Li}, e_{Ri}) = (\mathbf{3}, \mathbf{3})$  of  $U(3)$  family symmetry, because of  $\log M_{ii}^n = n \log M_{ii} < 0$  with the negative  $n$ .

In this paper, we call the extended FGB model Model A, and call the original model Model B. The characteristics of these models are summarized in Table 1. In order to relax the severe constraints from the observed  $P^0-\bar{P}^0$  mixings, we consider that the lightest FGB interacts with only the third generation quarks. We define the family-number as  $(e_1, e_2, e_3) = (e^-, \mu^-, \tau^-)$ . In Table 1, we list ‘‘optimistic’’ lower limit on  $M_{12}$  which is not conflict with all of observed  $P^0-\bar{P}^0$  mixings [4].

### 2.1. Model A

According to the extended FGB model, Model A is characterized by the following inverted mass hierarchy of FGB mass [3],

$$M_{ij}^2 \propto \frac{1}{m_{e_i}^n} + \frac{1}{m_{e_j}^n}, \quad (2.5)$$

( $n$  is a positive integer). Interaction Lagrangian of quarks and leptons with the FGBs is given by

$$\mathcal{L} = \frac{g_F}{\sqrt{2}} \left\{ \sum_{\ell=e,\nu} (\bar{\ell}^i \gamma_\mu \ell_j) + \sum_{q=u,d} U_{ik}^{q*} U_{jl}^q (\bar{q}^k \gamma_\mu q_l) \right\} (A^\mu)_i^j. \quad (2.6)$$

Here  $q_i^0 = U_{ij}^q q_j$  is an interaction eigenstate of the  $U(3)$  symmetry, where  $q_j$  and  $U_{ij}^q$  represent mass eigenstate and quark mixing matrix, respectively. The interactions are a type of pure vector, so that

the model is anomaly free. The gauge coupling  $g_F$  in Model A is given as [3]

$$\frac{g_F}{\sqrt{2}} = \left[ \frac{3\zeta}{2n} 4\pi \alpha_{em}(m_\mu) \right]^{1/2} = \frac{1}{\sqrt{n}} 0.491, \quad (2.7)$$

where  $\alpha_{em}(m_\mu) = 1/137$ , and  $\zeta = 1.752$  is a fine tuning factor which is obtained from phenomenological study.

## 2.2. Model B

Model B is characterized by the following relation of FGB mass,

$$M_{ij}^2 \propto m_{ei}^n + m_{ej}^n, \quad (2.8)$$

( $n$  is a positive integer). Interaction Lagrangian of quarks and leptons with the FGBs is given by

$$\begin{aligned} \mathcal{L} = & \frac{g_F}{\sqrt{2}} \left\{ \sum_{\ell=e,\nu} \left[ (\bar{\ell}_L^i \gamma_\mu \ell_{Lj}) - (\bar{\ell}_R^j \gamma_\mu \ell_R^i) \right] \right. \\ & \left. + \sum_{q=u,d} U_{ik}^{q*} U_{jl}^q (\bar{q}^k \gamma_\mu q_l) \right\} (A^\mu)_i^j. \end{aligned} \quad (2.9)$$

Here, note that the leptonic currents have an unfamiliar form,  $(V-A)_j^i - (V+A)_j^i$ , because fermions  $(\psi_L, \psi_R)$  are assigned to  $(\mathbf{3}, \mathbf{3}^*)$  of  $U(3)$ . Since this assignment in the quark sector leads unwelcome large  $K^0-\bar{K}^0$  mixing, we use pure vector current form as far as quark currents are concerned. The gauge coupling  $g_F$  is given by

$$\frac{g_F}{\sqrt{2}} = \left[ \frac{2}{n} 4\pi \alpha_{em}(m_\mu) \right]^{1/2} = \frac{1}{\sqrt{n}} 0.428. \quad (2.10)$$

In order to avoid the severe constraints from the observed  $P^0-\bar{P}^0$  mixing, the lightest FGB  $A_1^1$  couples only to the third generation quarks, so that we have the following two scenarios for the family-number assignment [4]:

$$\begin{aligned} (d_1, d_2, d_3) &= (b^0, s^0, d^0) \text{ in Model B}_1, \\ (d_1, d_2, d_3) &= (b^0, d^0, s^0) \text{ in Model B}_2. \end{aligned} \quad (2.11)$$

## 2.3. Typical cases of quark mixing

In the FGB model,  $\mu-e$  conversion branching ratio  $B(\mu^- N \rightarrow e^- N)$  is sensitive to the quark mixing matrices,  $U^u$  and  $U^d$ . Each explicit form is not determined yet, though the combination is measured as  $V_{CKM} = (U^u)^\dagger U^d$ . We calculate  $B(\mu^- N \rightarrow e^- N)$  by using some typical mixing matrices from the practical point of view.

The family numbers do not always correspond to the generation numbers in Model B. In order to avoid confusing, hereafter, we denote  $U^u, U^d$  and  $V_{CKM}$  in the generation basis and, e.g., we denote  $(U^d)_{12}$  as  $(U^d)_{ds}$ .

As the first case (Case I), we consider following mixing,

$$U^u \simeq \mathbf{1}, \quad U^d \simeq V_{CKM}, \quad (\text{Case I}). \quad (2.12)$$

Case I is the most likely case. Since we know  $m_t/m_u \gg m_b/m_d$ , we consider that the CKM mixing almost comes from down-quark mixing  $U^d$ . Besides, we know an empirical well-satisfied relation  $V_{us} \simeq \sqrt{m_d/m_s}$  without  $\sqrt{m_u/m_t}$  [17]. In fact, Case I is practically well satisfied in most of mass matrix models. We adopt the standard expression for the explicit form of  $V_{CKM}$ ,

$$\begin{aligned} V_{CKM} &= \begin{pmatrix} c_{13}c_{12} & c_{13}s_{12} & s_{13}e^{-i\delta} \\ -c_{23}s_{12} - s_{23}c_{12}s_{13}e^{i\delta} & c_{23}c_{12} - s_{23}s_{12}s_{13}e^{i\delta} & s_{23}c_{13} \\ s_{23}s_{12} - c_{23}c_{12}s_{13}e^{i\delta} & -s_{23}c_{12} - c_{23}s_{12}s_{13}e^{i\delta} & c_{23}c_{13} \end{pmatrix}, \end{aligned} \quad (2.13)$$

where  $(s_{12}, c_{12}) = (0.235, 0.974)$ ,  $(s_{23}, c_{23}) = (0.0412, 0.999)$ ,  $(s_{13}, c_{13}) = (0.00351, 1.000)$  and  $\delta = +72.2^\circ$  [18].

For comparison with Case I, we consider an opposite extreme case (Case II):

$$U^u \simeq V_{CKM}^\dagger, \quad U^d \simeq \mathbf{1}, \quad (\text{Case II}), \quad (2.14)$$

although such case is not likely in the realistic quark mass matrix model.

In addition to these cases, we investigate Case III, in which up- and down-quark mixings are sizable:

$$\begin{aligned} \tilde{U}^u &= \begin{pmatrix} 0.999 & 0.0320 e^{i8.14^\circ} & 0.0167 e^{i176^\circ} \\ 0.0351 e^{i172^\circ} & 0.970 & 0.242 e^{i168^\circ} \\ 0.00845 e^{i3.95^\circ} & 0.243 e^{i12.1^\circ} & 0.970 \end{pmatrix}, \\ \tilde{U}^d &= \begin{pmatrix} 0.977 & 0.212 e^{i119^\circ} & 0.0126 e^{i166^\circ} \\ 0.207 e^{i61.3^\circ} & 0.957 & 0.203 e^{i168^\circ} \\ 0.0506 e^{i60.8^\circ} & 0.197 e^{i12.6^\circ} & 0.979 \end{pmatrix}. \end{aligned} \quad (2.15)$$

The mixings in (2.15) have been derived in a mass matrix model [19] which is notable one: a unified description of the quark- and lepton-mixing matrices and mass ratios has been described by using only the observed charged lepton masses as family-number dependent parameters.

It is worth investigating the potential of the  $\mu-e$  conversion to determine the quark mixing. To do this, we consider Case IV with following parametrization:

$$U^u = R_3 \equiv \begin{pmatrix} \cos\theta & \sin\theta & 0 \\ -\sin\theta & \cos\theta & 0 \\ 0 & 0 & 1 \end{pmatrix}, \quad U^d = R_3^T V_{CKM}. \quad (2.16)$$

## 3. $\mu-e$ conversion in the FGB model

We formulate the reaction rate of  $\mu-e$  conversion in muonic atoms via  $A_2^1$  exchange based on Ref. [20]. Note that in the FGB model other muon lepton family violating (LFV) reactions ( $\mu \rightarrow e\gamma$ ,  $\mu \rightarrow 3e$ ,  $\mu^- e^- \rightarrow e^- e^-$  in muonic atom [21], and so on) arise at higher order. These reaction rates are suppressed by higher order couplings, gauge invariance, and so on. Hence we do not study these reactions here.

The  $\mu-e$  conversion via  $A_2^1$  exchange is described by the effective interaction Lagrangian,<sup>1</sup>

$$\begin{aligned} \mathcal{L}_{\text{int}} &= \left( \frac{g_F^X}{\sqrt{2}} \right)^2 \frac{1}{M_{12}^2} \\ &\times \sum_{q=u,d} \left\{ C_{L(q)}^{X,\alpha} (\bar{e}_L \gamma^\mu \mu_L) (\bar{q} \gamma_\mu q) C_{R(q)}^{X,\alpha} (\bar{e}_R \gamma^\mu \mu_R) (\bar{q} \gamma_\mu q) \right\}. \end{aligned} \quad (3.1)$$

Here  $X$  and  $\alpha$  denote the model,  $X \ni \{A, B_1, B_2\}$ , and the type of quark mixing matrices,  $\alpha \ni \{I, II, III, IV\}$ , respectively. The coefficients  $C_{L(q)}^{X,\alpha}$  and  $C_{R(q)}^{X,\alpha}$  are derived from interaction Lagrangian in

<sup>1</sup> We omit the contribution via the kinetic mixing of  $A_2^1$  and  $Z$  boson. The contribution is suppressed by the loop factor and quark mixings, and is sub-dominant relative to direct ones of  $A_2^1$ .

**Table 2**  
 $C_{L(u)}^{X,\alpha}$  and  $C_{L(d)}^{X,\alpha}$  for each model and for each quark mixing matrix.  $V_{qq'}$  and  $\tilde{U}^q$  stand for the CKM matrix and the mixing matrices derived in Ref. [19], respectively.

	Model A	Model B <sub>1</sub>	Model B <sub>2</sub>
$C_{L(u)}^{X,I}$	0	0	0
$C_{L(d)}^{X,I}$	$-V_{cd}^* V_{ud}$	$-V_{cd}^* V_{td}$	$-V_{ud}^* V_{td}$
$C_{L(u)}^{X,II}$	$-V_{us} V_{ud}^*$	$-V_{us} V_{ub}^*$	$-V_{ud} V_{ub}^*$
$C_{L(d)}^{X,II}$	0	0	0
$C_{L(u)}^{X,III}$	$-(\tilde{U}_{cu}^u)^* \tilde{U}_{uu}^u$	$-(\tilde{U}_{cu}^u)^* \tilde{U}_{tu}^u$	$-(\tilde{U}_{uu}^u)^* \tilde{U}_{tu}^u$
$C_{L(d)}^{X,III}$	$-(\tilde{U}_{sd}^d)^* \tilde{U}_{dd}^d$	$-(\tilde{U}_{sd}^d)^* \tilde{U}_{bd}^d$	$-(\tilde{U}_{dd}^d)^* \tilde{U}_{bd}^d$

**Table 3**

The overlap factor of wave functions and the muon capture rate  $\omega_{capt}$  for each nucleus  $N$ .

$N$	$V^{(p)}$	$V^{(n)}$	$\omega_{capt} (s^{-1})$
C	$3.12 \times 10^{-3}$	$3.12 \times 10^{-3}$	$3.88 \times 10^4$
Si	$1.87 \times 10^{-2}$	$1.87 \times 10^{-2}$	$8.71 \times 10^5$
Al	$1.61 \times 10^{-2}$	$1.73 \times 10^{-2}$	$7.05 \times 10^5$
Ti	$3.96 \times 10^{-2}$	$4.68 \times 10^{-2}$	$2.59 \times 10^6$
Au	$9.74 \times 10^{-2}$	$1.46 \times 10^{-1}$	$1.31 \times 10^7$
U	$7.98 \times 10^{-2}$	$1.27 \times 10^{-1}$	$1.24 \times 10^7$

**Table 4**

Lower bound on  $M_{12}$  for each quark mixing in each model from the  $\mu$ - $e$  conversion limit at SINDRUM-II,  $B(\mu^- \text{Au} \rightarrow e^- \text{Au}) < 7 \times 10^{-13}$  [22].

Case	Model A	Model B <sub>1</sub>	Model B <sub>2</sub>
I	291 TeV	24.2 TeV	50.4 TeV
II	273 TeV	14.4 TeV	29.8 TeV
III	273 TeV	54.8 TeV	126 TeV

each model discussed in previous section. We list  $C_{L(q)}^{X,\alpha}$  in the generation basis in Table 2.  $C_{R(q)}^{X,\alpha}$  is related with  $C_{L(q)}^{X,\alpha}$  as follows,

$$C_{R(u)}^{X,\alpha} = \begin{cases} +C_{L(u)}^{X,\alpha} & \text{for } X = A, \\ -C_{L(u)}^{X,\alpha} & \text{for } X = B_1 \text{ and } B_2, \end{cases} \quad (3.2)$$

$$C_{R(d)}^{X,\alpha} = \begin{cases} +C_{L(d)}^{X,\alpha} & \text{for } X = A, \\ -C_{L(d)}^{X,\alpha} & \text{for } X = B_1 \text{ and } B_2. \end{cases} \quad (3.3)$$

The branching ratio of  $\mu$ - $e$  conversion is defined by  $B(\mu^- N \rightarrow e^- N) = \omega_{conv}/\omega_{capt}$ , where  $\omega_{conv}$  and  $\omega_{capt}$  represent the reaction rates of  $\mu$ - $e$  conversion and of the muon capture process, respectively. The reaction rate  $\omega_{conv}$  is calculated by the overlap integral of wave functions of the initial muon, the final electron, and the initial and final nucleus. In the FGB model,  $\omega_{conv}$  is

$$\omega_{conv} = \left( \frac{g_F^X}{\sqrt{2}} \right)^4 \frac{4m_\mu^5}{M_{12}^4} \left| \left( 2C_{L(u)}^{X,\alpha} + C_{L(d)}^{X,\alpha} \right) V^{(p)} + \left( C_{L(u)}^{X,\alpha} + 2C_{L(d)}^{X,\alpha} \right) V^{(n)} \right|^2 + (L \leftrightarrow R). \quad (3.4)$$

Here  $m_\mu$  is the muon mass. The overlap integral of wave functions of muon, electron, and protons (neutrons) gives  $V^{(p)}$  ( $V^{(n)}$ ) (explicit formulae and details of the calculation are explained in Ref. [20]). We list  $V^{(p)}$  and  $V^{(n)}$  for relevant nuclei of SINDRUM-II (Au), DeeMe (C and Si), COMET (Al and Ti), Mu2e (Al and Ti), and PRISM (Al and Ti) in Table 3. We also list them for U nucleus. The  $\mu$ - $e$  conversion search with the U target can assist to confirm the FGB model and to determine the quark mixings.

#### 4. Numerical result

We are now in a position to show numerical results. Table 4 shows the lower bound on the FGB mass  $M_{12}$  by the  $\mu$ - $e$  con-

**Table 5**

$B(\mu^- \text{Al} \rightarrow e^- \text{Al})$  for each Case and Model. The values are given in a unit of  $n^{-2} (M_{12}/10^3 \text{ TeV})^{-4}$  for Model A, and  $n^{-2} (M_{12}/10^2 \text{ TeV})^{-4}$  for Model B.

Case	Model A	Model B <sub>1</sub>	Model B <sub>2</sub>
I	$8.54 \times 10^{-17}$	$7.54 \times 10^{-16}$	$1.42 \times 10^{-14}$
II	$1.51 \times 10^{-15}$	$1.14 \times 10^{-16}$	$2.22 \times 10^{-15}$
III	$1.22 \times 10^{-15}$	$1.94 \times 10^{-14}$	$5.64 \times 10^{-13}$

**Table 6**

$B(N)/B(\text{Al})$  in each model and for each quark mixing matrix. In Case I and II,  $B(N)/B(\text{Al})$  is universal for each model.

$N$	Case I	Case II	Case III (A)	Case III (B <sub>1</sub> )	Case III (B <sub>2</sub> )
Ti	1.88	1.77	1.88	1.88	1.87
C	0.620	0.650	0.619	0.619	0.623
Si	0.991	1.040	0.990	0.990	0.996
Au	3.18	2.56	3.21	3.20	3.12
U	2.47	1.91	2.49	2.48	2.41

version search at SINDRUM-II,  $B(\mu^- \text{Au} \rightarrow e^- \text{Au}) < 7 \times 10^{-13}$  [22]. Current most stringent limits of  $M_{12}$  are obtained from observed  $P^0$ - $\bar{P}^0$  oscillations (Table 1), not from the  $\mu$ - $e$  conversion search.

Next we show the feasibility of FGB search in  $\mu$ - $e$  conversion search experiments. Fig. 1 shows  $B(\mu^- \text{Al} \rightarrow e^- \text{Al})$  as a function of  $M_{12}$  (see also Table 5). In light of the cancellation, the FGB masses are supposed to be up to  $\sim 10^4$  TeV [1,2] (see Sec. 2). As is shown in Fig. 1, next generation experiments cover most of this mass region, and the discovery of  $\mu$ - $e$  conversion via  $A_2^1$  exchange is expected in near future. To put it the other way around null results of  $\mu$ - $e$  conversion search can rule out the FGB model.

After the discovery of  $\mu$ - $e$  conversion, we need to check whether the observed event is a signal of  $A_2^1$  or not. Table 6 lists the ratio of branching ratios,  $B(\mu^- N \rightarrow e^- N)/B(\mu^- \text{Al} \rightarrow e^- \text{Al})$ . The  $\mu$ - $e$  conversion events will be confirmed as the signal of  $A_2^1$  through precise measurements of the ratios. Also, a type of quark mixing matrix can be identified by the precise measurements. The  $\mu$ - $e$  conversion search by using large nucleus target is important. Indeed, although it is hard to distinguish the Case I and III(A) from the ratios  $B(\text{Ti})/B(\text{Al})$ ,  $B(\text{C})/B(\text{Al})$ , and  $B(\text{Si})/B(\text{Al})$ , it can be possible for large nucleus, i.e.,  $B(\text{Au})/B(\text{Al})$ , and  $B(\text{U})/B(\text{Al})$ . It is probably impossible to distinguish the Case III(A) and III(B<sub>1</sub>) from the ratios. To do this, we need additional observables via the FGB exchange, e.g., LFV kaon decays, LFV collider signals, and so on. Some of experiments are running or will launch in near future to search for these signals [23,24]. Therefore it is important to simulate what correlations are expected and how sensitivity is required for the purpose. It is however beyond the scope of this paper and we leave them in future work.

One may wonder why, in Table 6,  $B(N)/B(\text{Al})$  is insensitive to Model in Case I and II. This is understood as follows. The branching ratios can be decomposed into Model independent and dependent part as

$$B \propto \frac{1}{n^2} \frac{(g_F^X)^4}{M_{12}^4} \left| C_{L(d)}^{X,I} \right|^2 \left| V^{(p)} + 2V^{(n)} \right|^2 \quad (\text{Case I}), \quad (4.1)$$

$$B \propto \frac{1}{n^2} \frac{(g_F^X)^4}{M_{12}^4} \left| C_{L(u)}^{X,II} \right|^2 \left| 2V^{(p)} + V^{(n)} \right|^2 \quad (\text{Case II}). \quad (4.2)$$

For any target nuclei, the Model dependent part  $(g_F^X)^4 |C_{L(d)}^{X,I}|^2$  and  $(g_F^X)^4 |C_{L(u)}^{X,II}|^2$  are canceled in the ratio  $B(N)/B(\text{Al})$ . Hence, in Case I and II, the change in model does not affect the ratio.

Finally we discuss the determination of the quark mixing by using parametrized mixing matrix (2.19). The  $\theta$  dependence of  $B(\mu^- \text{Al} \rightarrow e^- \text{Al})$  is plotted in Figs. 2 (Model A,  $M_{12} = 1000$  TeV)

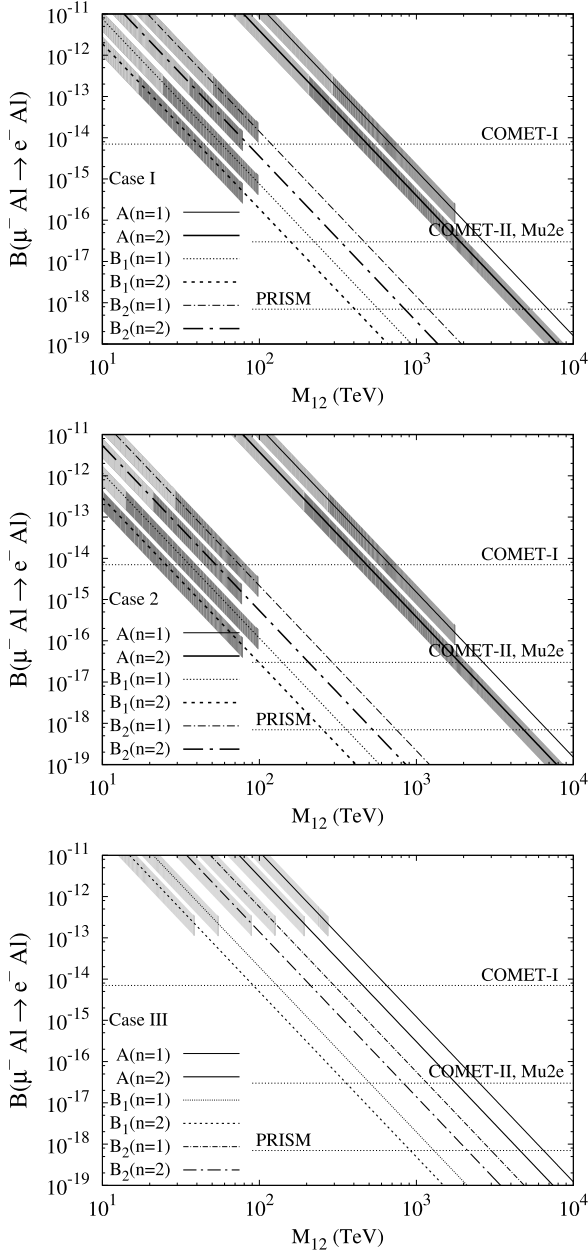


**Fig. 1.**  $M_{12}$  dependence of  $B(\mu^- \text{Al} \rightarrow e^- \text{Al})$  for  $U_u = \mathbf{1}$  and  $U_d = V_{\text{CKM}}$  (upper panel), for  $U_u = V_{\text{CKM}}^*$  and  $U_d = \mathbf{1}$  (middle panel), and for  $U^u = \tilde{U}^u$  and  $U^d = \tilde{U}^d$  (see Eq. (2.15)) (lower panel). Light and dark shaded region is excluded region by the SINDRUM-II and by the observed  $p^0\text{-}\bar{p}^0$  mixing (Table 1), respectively. Horizontal dashed lines show the single event sensitivities of each experiment (see Introduction).

and 3 (Model  $B_1$  and  $B_2$ ,  $M_{12} = 100$  TeV), respectively. The ratios  $B(N)/B(\text{Al})$  as a function of  $\theta$  are also shown in Fig. 2. The results at  $\theta = 0$  corresponds to those in Case I. The structure of mixing matrix can be determined through the precise measurement of  $B(\mu^- \text{Al} \rightarrow e^- \text{Al})$ . Particularly, in Model A, since the ratios  $B(N)/B(\text{Al})$  also depends on  $\theta$ , the quark mixing can be accurately determined by accumulating a large number of  $\mu$ - $e$  conversion events. Fig. 2 emphasizes an importance of the  $\mu$ - $e$  conversion searches with various target nuclei. In Model A, even if the signal of  $\mu^- \text{Al} \rightarrow e^- \text{Al}$  will never be found, a number of events can be observed at experiments with other target nucleus. On the other hand, in Models  $B_1$  and  $B_2$ , the ratios  $B(N)/B(\text{Al})$  are independent of  $\theta$ , and are equal to those of Case I. This is because that the

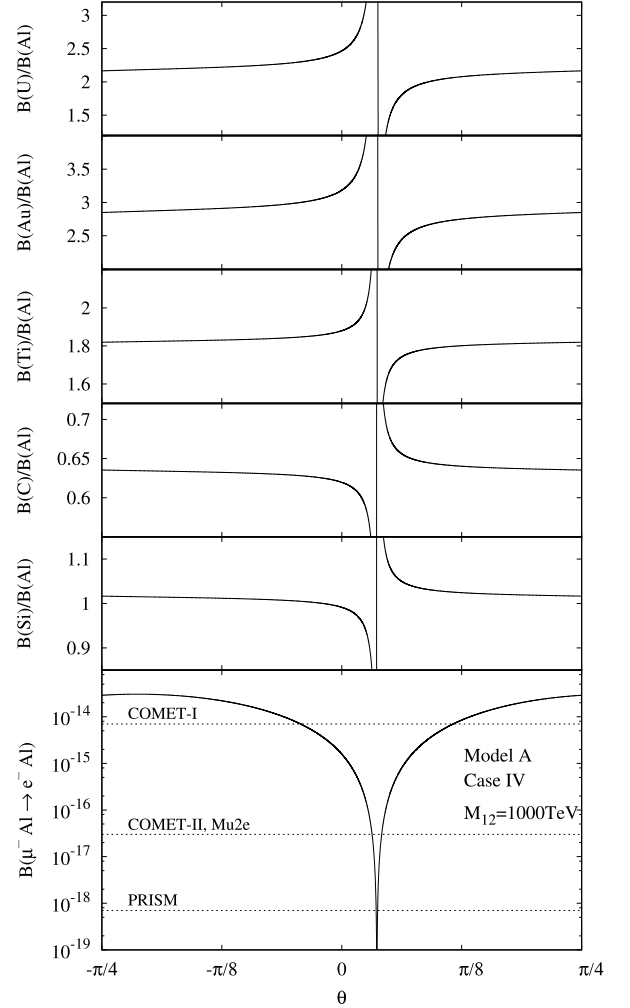


**Fig. 2.**  $\theta$  dependence of  $B(\mu^- \text{N} \rightarrow e^- \text{N})/B(\mu^- \text{Al} \rightarrow e^- \text{Al})$  in the model A. We took  $M_{12} = 1000$  TeV. Horizontal dashed lines show the single event sensitivities of each experiments (see Introduction).

branching ratios can be decomposed into  $\theta$  dependent part and independent part as follows

$$B_{(B_1)} \propto |V^{(p)} + 2V^{(n)}|^2 |(V_{ud}^* \sin \theta + V_{cd}^* \cos \theta) V_{td}|^2, \quad (4.3)$$

$$B_{(B_2)} \propto |V^{(p)} + 2V^{(n)}|^2 |(V_{ud}^* \cos \theta - V_{cd}^* \sin \theta) V_{td}|^2, \quad (4.4)$$

and the  $\theta$  dependent part is canceled in  $B(N)/B(\text{Al})$ . Thus, in Models  $B_1$  and  $B_2$ , it is difficult to examine the structure by the  $\mu$ - $e$  conversion search only. In such a case, it is necessary to combine the  $\mu$ - $e$  conversion search with other observables.

## 5. Concluding remarks

We have investigated the  $\mu$ - $e$  conversion via an exchange of family gauge boson  $A_2^1$  in a  $U(3)$  FGB model. In the model there are various types of FGB spectrum and of family-number assignments. We have considered three well-motivated models: a model with inverted family-number assignment (Model A), and models with twisted ones (Model  $B_1$  and  $B_2$ ). We also have a degree of freedom of choice of quark mixing  $U^u$  and  $U^d$ . We have introduced four types of mixing: a most likely mixing,  $U^u \simeq \mathbf{1}$  and  $U^d \simeq V_{\text{CKM}}$  (Case I), an opposite type of Case I,  $U^u \simeq V_{\text{CKM}}^\dagger$  and  $U^d \simeq \mathbf{1}$  (Case II), a phenomenologically derived mixing (2.15),  $U^u \simeq \tilde{U}^u$

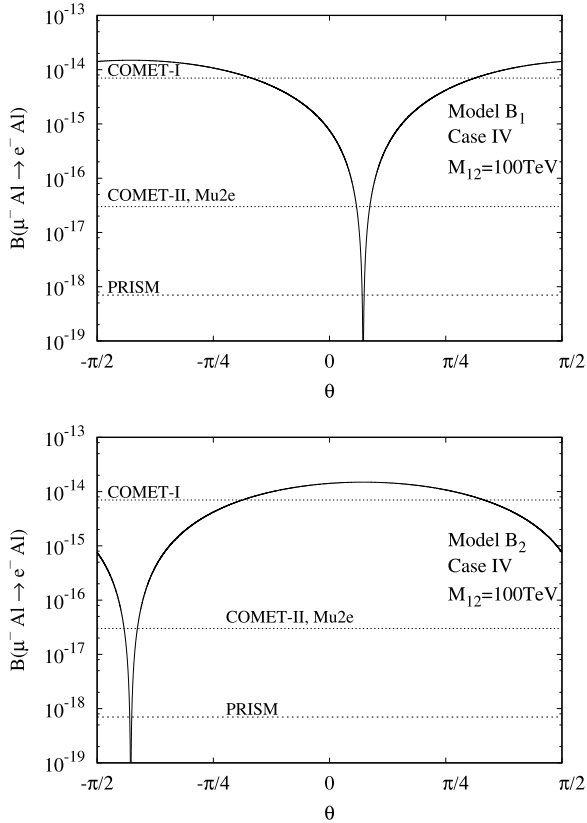


**Fig. 3.**  $\theta$  dependence of  $B(\mu^- \text{Al} \rightarrow e^- \text{Al})$  in the model  $B_1$  (upper plot) and in the model  $B_2$  (lower plot). Horizontal dashed lines show the single event sensitivities of each experiments (see Introduction).

and  $U^d \simeq \tilde{U}^d$  (Case III), and a parametrized mixing,  $U^u = R_3$  and  $U^d = R_3^T V_{\text{CKM}}$  (Case IV).

We have calculated the branching ratio of  $\mu$ - $e$  conversion process,  $B(\mu^- N \rightarrow e^- N)$ , in Models A,  $B_1$  and  $B_2$  for each type of quark mixing. We have shown that next generation  $\mu$ - $e$  conversion search experiments will cover entire energy scale of the FGB model, and could confirm or rule out the FGB model. Muon-number violating decays except for the  $\mu$ - $e$  conversion is extremely suppressed in the FGB model. Thus we have emphasized the importance of precise measurements of the ratios  $B(N)/B(\text{Al})$ , which is necessary to confirm the FGB model. Searches for LFV decays of mesons should assist the confirmation. This interesting possibility is left for future work.

In the FGB model it is, in principle, possible to individually determine quark mixing matrix  $U^u$  and  $U^d$ , in contrast within the SM. However, since  $V^{(p)} \simeq V^{(n)}$  in the most nuclei, it is hard to observe the difference between  $U^u$  and  $U^d$ . We hope that further precise search for the  $\mu$ - $e$  conversion with heavy nuclei, e.g., Au and/or U which  $V^{(p)}$  and  $V^{(n)}$  are sizably different.

### Acknowledgements

This work was supported by the Grants-in-Aid for Scientific Research (KAKENHI) Grant No. 16K05325 (Y.K.) and No. 16K05325 and No. 16K17693 (M.Y.).

### References

- [1] Y. Sumino, Phys. Lett. B 671 (2009) 477.
- [2] Y. Sumino, J. High Energy Phys. 0905 (2009) 075.
- [3] Y. Koide, T. Yamashita, Phys. Lett. B 711 (2012) 384.
- [4] Y. Koide, Phys. Lett. B 736 (2014) 499.
- [5] Y. Koide, M. Yamanaka, H. Yokoya, Phys. Lett. B 750 (2015) 384.
- [6] H. Natori, DeeMe Collaboration, Nucl. Phys. B, Proc. Suppl. 248–250 (2014) 52.
- [7] Y. Kuno, COMET Collaboration, Prog. Theor. Exp. Phys. 2013 (2013) 022C01.
- [8] L. Bartoszek, et al., Mu2e Collaboration, arXiv:1501.05241 [physics.ins-det].
- [9] D.N. Dinh, A. Ibarra, E. Molinaro, S.T. Petcov, J. High Energy Phys. 1208 (2012) 125; Erratum: J. High Energy Phys. 1309 (2013) 023.
- [10] R. Alonso, M. Dhen, M.B. Gavela, T. Hambye, J. High Energy Phys. 1301 (2013) 118.
- [11] T. Toma, A. Vicente, J. High Energy Phys. 1401 (2014) 160.
- [12] A. Abada, M.E. Krauss, W. Porod, F. Staub, A. Vicente, C. Weiland, J. High Energy Phys. 1411 (2014) 048.
- [13] J. Sato, M. Yamanaka, Phys. Rev. D 91 (2015) 055018.
- [14] N. Cabibbo, Phys. Rev. Lett. 10 (1963) 531; M. Kobayashi, T. Maskawa, Prog. Theor. Phys. 49 (1973) 652.
- [15] Y. Koide, Lett. Nuovo Cimento 34 (1982) 201; Phys. Lett. B 120 (1983) 161; Phys. Rev. D 28 (1983) 252.
- [16] H. Arason, et al., Phys. Rev. D 46 (1992) 3945.
- [17] S. Weinberg, Ann. N.Y. Acad. Sci. 38 (1977) 185; H. Fritzsch, Phys. Lett. B 73 (1978) 317; H. Georgi, D.V. Nanopoulos, Nucl. Phys. B 155 (1979) 52.
- [18] K.A. Olive, et al., Particle Data Group Collaboration, Chin. Phys. C 38 (2014) 090001.
- [19] Y. Koide, H. Nishiura, Phys. Rev. D 92 (11) (2015) 111301(R); Mod. Phys. Lett. A (2016) 1650125.
- [20] R. Kitano, M. Koike, Y. Okada, Phys. Rev. D 66 (2002) 096002; R. Kitano, M. Koike, Y. Okada, Phys. Rev. D 76 (2007) 059902 (Erratum).
- [21] M. Koike, Y. Kuno, J. Sato, M. Yamanaka, Phys. Rev. Lett. 105 (2010) 121601.
- [22] W.H. Bertl, et al., SINDRUM II Collaboration, Eur. Phys. J. C 47 (2006) 337.
- [23] The ATLAS Collaboration, ATLAS-CONF-2015-072.
- [24] A. Sher, et al., Phys. Rev. D 72 (2005) 012005.